Asian Research Journal of Mathematics

Volume 19, Issue 8, Page 28-46, 2023; Article no.ARJOM.99830
ISSN: 2456-477X

Vibration Study of Rotating Rigid Hub and a Flexible Composite Beam under Simultaneous Primary-internal Resonance

M. Kamel [a++*], H. El-Gohary [a#], H. M. Shawky [b++] and H. Mosaa [b†]

[a] *Department of Physics and Engineering Mathematics, Faculty of Electronic Engineering, Menouf, Menoufia University, Egypt.*
[b] *Department of Mathematics, Faculty of Science, Al-Azhar University, (Girl's Branch), Egypt.*

Authors' contributions

This work was carried out in collaboration among all authors. All authors read and approved the final manuscript.

Article Information

DOI: 10.9734/ARJOM/2023/v19i8685

Open Peer Review History:
This journal follows the Advanced Open Peer Review policy. Identity of the Reviewers, Editor(s) and additional Reviewers, peer review comments, different versions of the manuscript, comments of the editors, etc are available here: https://www.sdiarticle5.com/review-history/99830

Original Research Article

Received: 09/03/2023
Accepted: 12/05/2023
Published: 22/05/2023

Abstract

In this paper, the vibration of a composite system consisting of a rotating rigid hub and a flexible thin-walled beam is considered and studied. The equation of motion is derived in the previous work of Warminski and Latalski. The method of multiple scale technique has been applied to obtain frequency response equations near the simultaneous internal and primary resonance case in the absence of the acceleration of the hub. The vibration stability at this resonance case is investigated from the frequency response equations and studied using Liapunov's methods. The effects of changes in selected structural parameters on the vibrating system behavior are investigated and studied numerically. Through the performed studies of the effects of changes in

[++] *Professor;*
[#] *Assistant Professor;*
[†] *Lecture Assistant;*
Email: hebaelsayed.elrc@gmail.com;

selected system a shift of the steady state amplitudes and the multi-valued of the bent curves are observed and the steady state amplitudes of the beam and hub have decreasing in the instability regions for natural frequencies. Finally, a comparison with the papers of previously published work is reported.

Keywords: Simultaneous primary resonance; frequency response curves; system stability; jump phenomenon.

1 Introduction

The dynamics of rotating beams are widely used in many applications such as flexible manipulators, thin and long wind turbine blades, helicopter rotor blades, rotating blades in turbo machinery, locomotive electrical generators and turbine engine blades. In most of these applications the base excitation take the form of a translational acceleration and affect the overall performance of the rotating structure. So, most of these structures may exhibit complicated dynamics and the increased lateral blade vibrations lead to the large responses and the dynamic instability phenomenon. Research work concerning vibration of the coupled bending-torsional problems has been carried out by [1-4].

Fundamental work regarding vibrations of such a structure were attributed to many authors. Lee and Sheu [5], discussed the vibration of two coupled differential equations for a rotating inclined beam. The vibration system was considered as the superposition of a static subsystem and a dynamic subsystem and the method of Frobenius was used to establish the exact series solutions of the system. The numerical results illustrated the influence of the physical parameters on the natural frequencies of the dynamic system. Wen and Kuo [6], investigated the natural frequency of the flawise bending vibration, coupled lagwise bending and axial vibration for the rotating beam. The rotating beam was subdivided into several equal segments and the governing equations of each segment were solved by a power series. Numerical examples were studied to demonstrate the accuracy and efficiency of the proposed method. Kamel and Amer [7] simulated the vibration of a cantilever beam under multi parametric excitation forces. They applied the multiple scales method to obtain the frequency response equations and to study the steady state solution of the sub-harmonic excitation system. Effects of the different parameters on the system behavior were also investigated. Kamel et al. [8] was studied also the nonlinear non-planar oscillations of a cantilever beam under multi external and multi parametric excitation forces. This system was analyzed using multiple scales method and the steady state response and its stability near the simultaneous sub-harmonic solution was obtained and studied. The numerical solutions were focused on both the effects of different parameters on the frequency response curve and the behavior of the system at resonant conditions.

Research work of the vibration analyses of rotating beams were reported in the work by [9-11]. They have been made to study the effect of a non-linear constraint on simply supported and rotating beams, respectively. In this context many researchers have investigated the dynamic characteristics of rotating blades and rotor structures [12–16]. Petrovet et al. [12] analyzed the multi-harmonic forced response large-scale finite element models of bladed disks taking into account the nonlinear forces acting at the contact interfaces of blade roots. Examples of application to the analysis of root damping and forced response levels were given and numeric al investigations of effects of contact conditions at root joints and excitation levels were explored for practical bladed disks. He et al. [13] studied the forced vibration response of a simplified turbine blade with a new kind of under-platform dry friction dampers. The vibrations of the two dampers, and the horizontal and transverse platform vibrations were coupled by friction at the contact interfaces. The Finite Element method and Modal Superposition were applied to solve the dynamic response and quasi-periodic vibration is found even under harmonic excitation. Qin et al. [14] studied the fundamental understanding about the influence of the bolt loosening at the rotating joint interface on the rotor dynamics, which are helpful for the bolt loosening detection of rotating components in heavy-duty rotating machinery. Also, Qin et al. [15] studied the vibration analysis of a rotating cylindrical shell coupled with an annular plate. The equations of motion for the rotating shell-plate combination were derived by taking Chebyshev polynomials as the admissible functions and the Rayleigh–Ritz method. They also, evaluated the effects of the geometric parameters and the boundary and coupling conditions on the vibration behavior of the coupled structure. Li et al. [16] established a dynamic model of a rotor-blade system considering the effect of nonlinear supports at both ends. The nonlinear vibration and stability of the system were studied by multiple scales method. The results show that the original hardening type of nonlinearity may be enhanced or transformed into softening type due to the positive or negative nonlinear stiffness terms of the bearing and withe increase in rubbing force and support stiffness, the jump-down frequency, resonant peak and the frequency range in which

the system has unstable responses increase. Furthermore, Cao et al. [17] investigated a dynamical equation of motion for a rotational cantilever flexible blade in a centrifugal force field and applied Galerkin method to discretize the partial differential equations to a 3-DOF system so as to compute the dynamic responses of the aero-engine blade constrained by friction interfaces due to tip-rub. These equations have been solved numerically and several results related to damped vibration characteristics of the blade with regard to rotational speed and gap were numerically obtained. Also, Cao et al. [18] developed a new structural dynamic model to study the free vibration characteristics of pre-twisted rotating functionally graded sandwich blades. The effects of frequency parameters such as the twist angle, the thickness ratio, the aspect ratio, the layer thickness ratio, the scalar parameter of volume fraction, the stagger angle, and the rotation velocity on the vibration characteristics were investigated. Furthermore, frequency locus veering and mode shape exchanging phenomena were found both in both static and dynamic states.

Different types of composite beam structures were generally used in different applications and in most of these applications the base excitation take the form of a translational acceleration and affect the overall performance of the rotating structure. Das et al. [19] investigated the free, out-of-plane vibration of a rotating beam with a non-linear spring–mass system. The solution of the resulting non-linear partial differential equations and the boundary conditions have been obtained applying the method of multiple time-scales. Subsequent non-linear study indicated that there was a pronounced effect of the spring and its mass and the influence of the spring–mass location on frequencies of the rotating beam was investigated. Xue and Tang [20] developed a general methodology for the vibration control of a nonlinear rotating beam. An integral sliding mode approach was proposed for the vibration control of the system with nonlinear coupling effect between the hub rotation and the beam transverse vibration. This integral sliding mode control is continuous in nature, which can alleviate or avoid the chattering problem. A series of simulation studies demonstrated that the proposed control method can effectively suppress the beam vibration induced by the hub rotation and the external disturbance. The dynamic characteristics of a rotating beam played a significant role in the overall performance and design of various engineering systems. Pohit et al. [21-23] investigated the effect of non-linear elastomeric constraint on a rotating blade of the modeled the characteristics of an elastomeric material. A numerical perturbation technique has been applied to determine the frequency–amplitude relationship of a rotating beam under transverse vibration. The free flexural-longitudinal vibrations of rotating beams and derived a system of ordinary differential equations which were analyzed and studied using the nonlinear normal modes by Peshek et al. [10]. Avramov et al. [24,25] derived and analyzed the nonlinear flexural-flexural-torsional vibrations of asymmetric cross-sections rotating beams without and with the center of gravity and shear centre. Suitable expansion in terms of modes of coupled flexural-torsional vibrations have been used to simulate the beam vibrations and the free vibration was studied by using nonlinear normal mode.

The equations of motion of composite Timoshenko beam experiencing variable angular velocity were derived and studied by several researchers. Dakel et al. [26] studied the dynamic behavior of a rotor in the presence of base excitations. They proposed the rotor model based on the Timoshenko beam finite element, taking into account the rotary inertia, gyroscopic inertia, and shear deformation of the shaft as well. Moreover, Quasi-analytical and numerical solutions for symmetric and asymmetric rotor configurations were given by means of stability charts, Campbell diagrams, steady state responses as well as orbits of the rotor. Arvin et al. [27], investigated and studied the linear and nonlinear free vibrations of rotating compositeTimoshenko beams. The Galerkin discretization approach has been applied to the linearized updated equations of motion to determine the linear normal modes and the associated natural frequencies of the rotating composite Timoshenko beam.The Galerkin discretization approach was applied to the linearized updated equations of motion to determine the linear normal modes and the associated natural frequencies of the rotating composite Timoshenko beam. Also, Georgiades et al. [28], studied and derived equations of motion of a rotating composite Timoshenko beam utilizing the Hamilton principle. A consequence of terms related to non-constant rotating speed was presented and they showed that both the variable rotating speed and nonzero pitch angle have significant impact on systems dynamics.

Recently, a lot of scientists have been focused on the investigation on the mechanical, thermal behavior of the functionally graded sandwich plates and functionally graded materials (FGM) which are extremely used in the engineering and industry. Luat et al. [29] presented a study of a refined simple shear deformation theory in combination with nonlocal elastic theory to investigate the bending, free vibration and buckling of novel bi-functionally graded sandwich nanobeams. They derived and solved the equations of motion of simply supported nanobeams by using the Hamilton principle and closed-form solution based on Navier's method. Their outcomes

of this study can serve as benchmarks for the future works on the bending, free vibration and buckling response of the bi-FGSW beams, plates and shells. Thom et al. [30] introduced a novel numerical outcomes of vibration response analysis of cracked FGM plate based on phase-field theory and finite element method. The finite element formulations are derived based on first order shear deformation Mindlin plate theory. Their numerical outcomes demonstrated that the stiffeners have a powerful impact on the free vibration of the structure. These computed data can be stratified for engineers when analyzing and designing these kinds of structures in practice. Also, the nanoplates have been utilized widely in electronic device [31,32]. Wang and Fang [31] used the classical plate theory and an analytical solution to demostrate the free vibration of nanoplates under the consideration of both static and dynamic flexoelectricit. Duc et al. [32] based the free vibration and static buckling of nanoplates by using a shear deformation theory with the finite element method and the phase-field theory. The efficiency of their study was increased when taking into account the impact of flexoelectricity. Their calculation outcomes extremely help the design, fabrication and practical utilize of nanoscale structures.

For multi-layer and three-layer composite beam plates play a very crucial role in the mechanical behavior of the beam. Nguyen et al. [33,34] presented a new study of equations of triple-layer composite plates with layers connected by shear connectors under moving load utilizing Mindlin's theory and finite element modelling. They reached by numerical tests to minimize plate oscillation. Moreover [34], the authors discussed the free vibration response and static bending of cracked composite plates utilizing third-order shear deformation theory and phase-field theory. They solved the equation of motions by using the finite element method. The phase-field theory is a new method for simulating fracture issues.

In this paper, a two degree of freedom system consisting of the rotating beam and the hub system subjected to external force is considered and studied and the dynamics of a thin-walled cantilever beam with a rigid hub performing motions of rotation and in plane translation. Our work is an extension and at the same time, a specification of the previous work of Warminski et al. [35,36]. The forced vibrations are examined under periodic excitation f and without translational motion $\ddot{\xi} = 0$. The multiple scale perturbation technique is applied to derive the steady state equation and amplitude-phase modulating equations. In the absence of the acceleration of the hub the stability of the steady state solution near the simultaneous primary resonance is investigated and studied by applying Liapunov's methods. The effects of different system parameters on the frequency response curve are studied. The numerical solutions are performed to validate the accuracy of the approximate results and enabled us to obtain the jump phenomenon of the hub and the beam system and to study curve bending of the steady state solution.

2 System Model and Mathematical Analysis

The system of slender, straight and elastic composite thin-walled beam clamped at the rigid hub is shown in Fig. 1, is experiencing rotational motion as well as translational one. The nonlinear differential equations that describe the motion of the given system subjected to harmonic excitation force is given as [35,36].

$$\ddot{Z}(t) + \varepsilon\mu_1\dot{Z}(t) + \omega_1^2 \mathrm{Z}(t) + \varepsilon\alpha_{12}\ddot{\psi}(t) + \varepsilon\alpha_{13}(\dot{\psi}(t))^2 \mathrm{Z}(t) + \varepsilon\alpha_{14}\dot{\psi}(t)\dot{\mathrm{Z}}(t) + \varepsilon\beta_{11}\ddot{\xi}\,\mathrm{Z}(t)\cos\psi + \varepsilon\beta_{12}\ddot{\xi}\sin\psi = 0 \quad (1a)$$

$$\ddot{\psi}(t) + \varepsilon\mu_2\dot{\psi}(t) + \omega^2\psi(t) + \varepsilon\alpha_{21}\ddot{\psi}(t)\,\mathrm{Z}(t) + \varepsilon\alpha_{22}\ddot{Z}(t) + \varepsilon\alpha_{23}\dot{\psi}(t)\,\dot{\mathrm{Z}}(t) + \varepsilon\beta_{21}\ddot{\xi}\,\mathrm{Z}(t)\cos\psi + \varepsilon\beta_{22}\ddot{\xi}\sin\psi = \varepsilon f\,\cos(\Omega t) + \varepsilon\,\mathrm{p}\psi(t) \quad (1b)$$

Where Z, ψ are the generalized coordinate of the studied coupled flexural-torsional motion of thin-walled beam and the hub system, μ_1, μ_2 are the damping coefficients of the beam and the hub respectively, ω_1, ω are the natural frequency of the beam and the hub. Coefficients of $(\alpha_{12}, \alpha_{13}, \alpha_{14})$ and $(\alpha_{21}, \alpha_{22}, \alpha_{23})$ are the non-linear parameters of the beam and the hub system. $\beta_{ij}\,(i, j = 1, 2)$ are characteristic parameters of the beam

and the hub, $\ddot{\xi}$ is the acceleration of the hub, p is a linear parameter of the hub ($\omega^2 = \varepsilon p$), f and Ω are the external excitation force and frequency of the hub system and ε is small perturbation parameter.

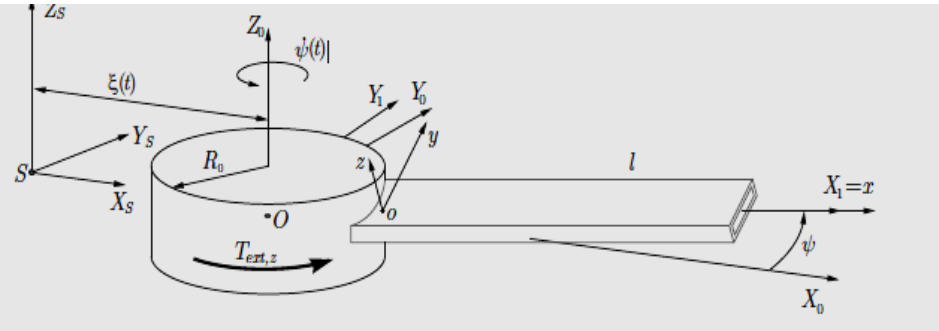

Fig. 1. The model of rotating thin-walled beam and the hub

By applying the multiple scales perturbation technique [37,38],we can obtain first-order approximate solutions to Eqs. (1a) and (1b) by seeking solutions in the following form:

$$Z(t;\varepsilon) = z_0(T_0,T_1) + z_1(T_0,T_1) + O(\varepsilon^2) \tag{2a}$$

$$\psi(t;\varepsilon) = \psi_0(T_0,T_1) + \psi_1(T_0,T_1) + O(\varepsilon^2) \tag{2b}$$

where $T_0 = t$ and $T_1 = \varepsilon t$ are the fast and slow time scales respectively, the time derivatives are transformed into

Substituting equations (2a), (2b) and (3) into equations (1a) and (1b), and equating the coefficients of the same power of ε in both sides, we get the following system of differential equations:

$$\frac{d}{dt} = D_0 + \varepsilon D_1, \quad \frac{d^2}{dt^2} = D_0^2 + 2\varepsilon D_0 D_1 \tag{3}$$

$$O(\varepsilon^0): (D_0^2 + \omega_1^2) z_0 = 0 \tag{4a}$$

$$(D_0^2 + \omega^2)\psi_0 = 0 \tag{4b}$$

$$O(\varepsilon): (D_0^2 + \omega_1^2) z_1 = -2D_0D_1z_0 - \mu_1(D_0 z_0) - \alpha_{12}(D_0^2\psi_0) - \alpha_{13}(D_0\psi_0)^2 z_0 - \alpha_{14}(D_0\psi_0)(D_0 z_0) \tag{5a}$$

$$(D_0^2 + \omega^2)\psi_1 = -2D_0D_1\psi_0 - \mu_2(D_0\psi_0) - \alpha_{21}(D_0^2\psi_0) z_0 - \alpha_{22}(D_0^2 z_0) - \alpha_{23}(D_0\psi_0)(D_0 z_0) + f\cos\Omega t + p\psi_0 \tag{5b}$$

$$z_0 = A_0 \exp(i\omega_1 T_0) + \bar{A}_0 \exp(-i\omega_1 T_0) \tag{6a}$$

$$\psi_0 = B_0 \exp(i\omega T_0) + \bar{B}_0 \exp(-i\omega T_0) \tag{6b}$$

The general solutions of Eqs. (4a) and (4b) can be written in the form:

Where $A_0, \bar{A}_0, B_0, \bar{B}_0$ are denote unknown functions in T_1, which can be determined from eliminating the secular terms at the next approximation, and the bar stands for the complex conjugate of the preceding functions. Inserting equations (6a), (6b) into equations (5a) and (5b), the following are obtained:

$$(D_0^2+\omega_1^2)\mathrm{z}_1=[-2i\,\omega_1 D_1 A_0-i\,\omega_1\mu_1 A_0-2\alpha_{13}\omega^2\,\mathrm{B}_0\bar{\mathrm{B}}_0\,A_0]\exp(i\,\omega_1 T_0)+[\alpha_{12}\omega^2 B_0]\exp(i\,\omega T_0)$$
$$+[\alpha_{14}\omega\omega_1 A_0 B_0]\exp(i\,(\omega_1+\omega)\,\mathrm{T}_0)-[\alpha_{14}\omega\omega_1 A_0\bar{B}_0]\exp(i\,(\omega_1-\omega)\,\mathrm{T}_0)$$
$$+[\alpha_{13}\omega^2 A_0 B_0{}^2]\exp(i\,(\omega_1+2\omega)\,\mathrm{T}_0)+[\alpha_{13}\omega^2 A_0\bar{B}_0{}^2]\exp(i\,(\omega_1-2\omega)\,\mathrm{T}_0)+\mathrm{cc} \quad (7a)$$

$$(D^2{}_0+\omega^2)\psi_1=[-2i\,\omega D_1 B_0-i\,\omega\mu_2 B_0+pB_0]\exp(i\,\omega T_0)+[\alpha_{22}\omega_1{}^2 A_0]\exp(i\,\omega_1 T_0)+[\frac{\mathrm{f}}{2}]\exp(i\,\Omega T_0)$$
$$+[\alpha_{21}\omega^2 A_0 B_0+\alpha_{23}\omega\omega_1 A_0 B_0]\exp(i\,(\omega_1+\omega)\,\mathrm{T}_0)$$
$$+[\alpha_{21}\omega^2 A_0\bar{B}_0-\alpha_{23}\omega\omega_1 A_0\bar{B}_0]\exp(i\,(\omega_1-\omega)\,\mathrm{T}_0)+\mathrm{cc} \quad (7b)$$

The general solution of the first approximation of equations (7) are given by:

$$z_1=A_1\exp(i\,\omega_1 T_0)+\mathrm{E}_1\exp(i\,\omega T_0)+\mathrm{E}_2\exp(i\,(\omega_1+\omega)T_0)+\mathrm{E}_3\exp(i\,(\omega_1-\omega)T_0)$$
$$+\mathrm{E}_4\exp(i\,(\omega_1+2\omega)T_0)+\mathrm{E}_5\exp(i\,(\omega_1-2\omega)T_0)+\mathrm{cc} \quad (8a)$$

$$\psi_1=B_1\exp(i\,\omega T_0)+H_1\exp(i\,\omega_1 T_0)+H_2\exp(i\,\Omega T_0)+H_3\exp(i\,(\omega_1+\omega)T_0)$$
$$+H_4\exp(i\,(\omega_1-\omega)T_0)+cc \quad (8b)$$

where $E_1,...,E_5$ and $H_1,...,\mathrm{H}_4$ are constant functions in T_1 (see Appendix-1).

Before we proceed to the next step of the analysis, the reported resonance cases at this approximation order are obtained as:

(a) Internal resonance: $\omega\cong\omega_1$. (b) Primary resonance: $\Omega\cong\omega$.

(c) Simultaneous or incident resonance: any combination of the above resonance cases.

2.1 Numerical results

The numerical solutions for the system of nonlinear differential equations (1), are obtained by applying Runge-Kutta forth order method and using Maple 16, as shown in Fig. 2 at the following selected parameters values.

$$\alpha_{22}=-0.160,\alpha_{23}=-0.0731,f=0.5 \quad ,$$
$$\omega_1=1.45,\Omega=0.5,\omega=0.1,p=0.1,\varepsilon=0.1,\alpha_{21}=-0.0731,$$
$$\mu_1=0.01807,\mu_2=0.05,\alpha_{12}=-2.9063,\alpha_{13}=0.3527,\alpha_{14}=0.4602$$

From Fig. 2, we have the steady state response for the non-resonant system at some practical values of the equations parameters. The rotating beam $\boldsymbol{Z}$ is about 3% of the external excitation force f **,** and the amplitude of the rotating beam $\boldsymbol{Z}$ is decreasing with some chaos, while the amplitude of the hub system ψ for is about 50% of the external excitation force.

Some different resonance cases are confirmed numerically as shown in Fig. 3. From these figures we find the worst resonance case is the simultaneous internal and primary resonance $\omega=\omega_1,\Omega\cong\omega$,where the steady state response of the rotating beam z is about 2000% of the external excitation force (f) and the amplitude of the hub system ψ is about 120% of the external excitation force (f).

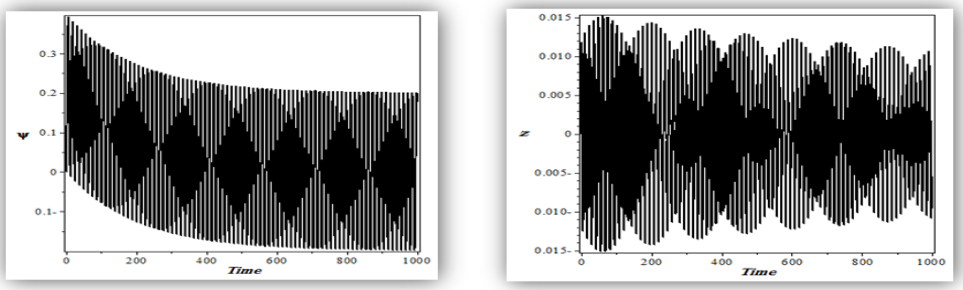

Fig. 2. Response of the basic case of the rotating beam and hub system

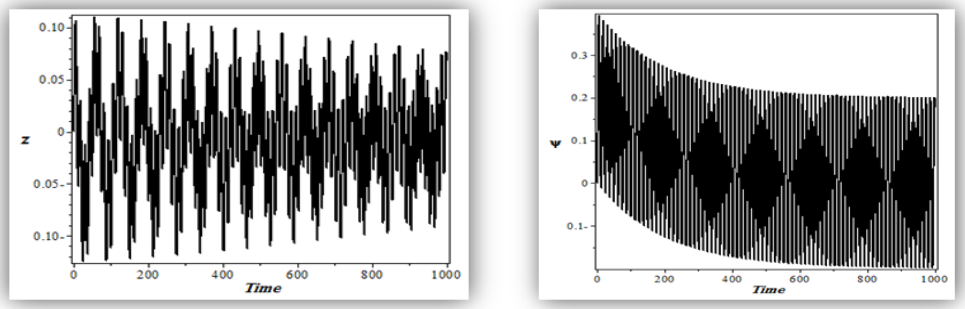

Fig. 3a. System behavior at internal resonance case $\omega \cong \omega_1$

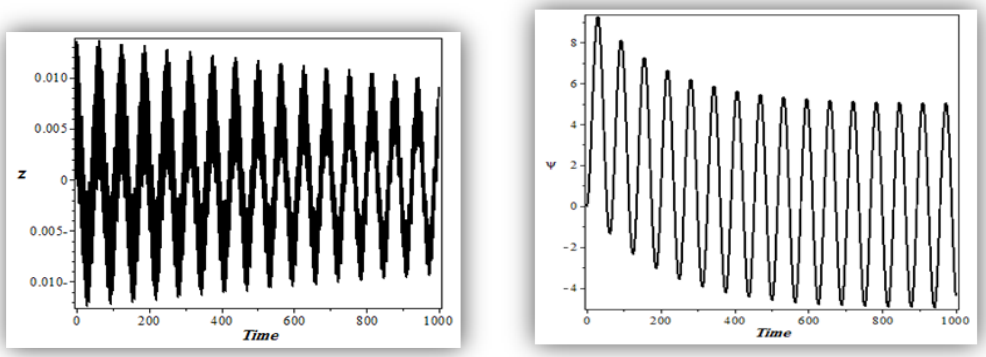

Fig. 3b. System behavior at primary resonance case $\Omega \cong \omega$

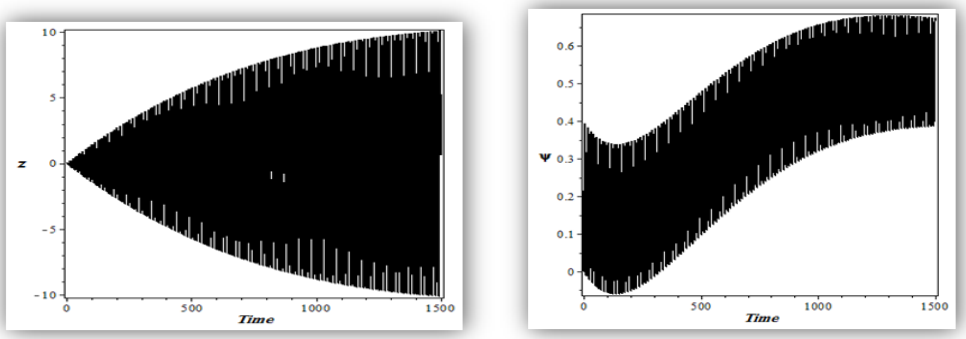

Fig. 3c. System behavior at simultaneous resonance case $\omega = \omega_1, \Omega \cong \omega$

2.2 Steady state solution and stability analysis

The steady state amplitude of the considered system is investigated near the simultaneous resonance case $\omega = \omega_1, \Omega \cong \omega$ by introducing the two detuning parameters σ_1 and σ_2 to describe quantitatively the closeness of Ω and ω_1 to ω as follows

$$\omega \cong \omega_1 + \varepsilon\sigma_1 \text{ , } \Omega \cong \omega + \varepsilon\sigma_2 \tag{9}$$

Substituting equation (9) into the small-divisor and secular terms of equations (7), we get the following solvability conditions:

$$(-2\mathrm{i}\omega_1(\mathrm{D}_1\mathrm{A}_0) - \mathrm{i}\omega_1\mu_1 A_0 - 2\alpha_{13}\omega^2\,\mathrm{B}_0\bar{\mathrm{B}}_0\mathrm{A}_0)\exp(i\,\omega_1 T_0) + (\alpha_{13}\omega^2 {B_0}^2\bar{A}_0)\exp(-i\,(\omega_1 - 2\omega)T_0)$$
$$+(\alpha_{12}\omega^2 B_0)\exp(i\,\omega T_0) = 0 \tag{10a}$$

$$(-2\mathrm{i}\omega\mathrm{D}_1 B_0 - i\,\omega\mu_2\,\mathrm{B}_0 + \mathrm{pB}_0)\exp(i\,\omega T_0) + (\alpha_{22}{\omega_1}^2 A_0)\exp(i\,\omega_1 T_0) + \frac{f}{2}\exp(i\,\Omega T_0) = 0 \tag{10b}$$

To analyze equations (10), we write $A_0(T_1)$ and $B_o(T_1)$ in the polar form

$$A_0 = \frac{1}{2}a_1(T_1)e^{i\,\gamma_1(T_1)}, \quad B_0 = \frac{1}{2}a_2(T_1)e^{i\,\gamma_2(T_1)} \tag{11}$$

Where a_1 and a_2 are the steady-state amplitudes of the motion of the rotating beam and the hub respectively, and γ_1, γ_2 are the phases of the motion. Inserting equation (11) into equations (10) and separating the real and imaginary parts we obtain:

$$\dot{a}_1 = -\frac{\mu_1 a_1}{2} + \frac{\alpha_{12}\omega^2 a_2}{2\omega_1}\sin(\phi_2) + \frac{\alpha_{13}\omega^2 a_1 {a_2}^2}{8\omega_1}\sin(2\phi_2) \tag{12a}$$

$$a_1\dot{\gamma}_1 = \frac{\alpha_{13}\omega^2 a_1 {a_2}^2}{4\omega_1} - \frac{\alpha_{13}\omega^2 a_1 {a_2}^2}{8\omega_1}\cos(2\phi_2) - \frac{\alpha_{12}\omega^2 a_2}{2\omega_1}\cos(\phi_2) \tag{12b}$$

$$\dot{a}_2 = -\frac{\mu_2 a_2}{2} - \frac{\alpha_{22}{\omega_1}^2 a_1}{2\omega}\sin(\phi_2) + \frac{f}{2\omega}\sin(\phi_1) \tag{12c}$$

$$a_2\dot{\gamma}_2 = -\frac{pa_2}{2\omega} - \frac{\alpha_{22}{\omega_1}^2 a_1}{2\omega}\cos(\phi_2) - \frac{f}{2\omega}\cos(\phi_1) \tag{12d}$$

where $\phi_1 = \sigma_2 T_1 - \gamma_2$, $\phi_2 = \sigma_1 T_1 + \gamma_2 - \gamma_1$

For steady-state solutions, we have $\dot{a}_1 = \dot{a}_2 = \dot{\phi}_1 = \dot{\phi}_2 = 0$, and equations (12) become in the form

$$\frac{\mu_1 a_1}{2} = \frac{\alpha_{12}\omega^2 a_2}{2\omega_1}\sin(\phi_2) + \frac{\alpha_{13}\omega^2 a_1 a_2{}^2}{8\omega_1}\sin(2\phi_2) \tag{13a}$$

$$-(a_1(\sigma_1+\sigma_2) - \frac{\alpha_{13}\omega^2 a_1 a_2{}^2}{4\omega_1}) = \frac{\alpha_{13}\omega^2 a_1 a_2{}^2}{8\omega_1}\cos(2\phi_2) + \frac{\alpha_{12}\omega^2 a_2}{2\omega_1}\cos(\phi_2) \tag{13b}$$

$$\frac{\mu_2 a_2}{2} = -\frac{\alpha_{22}\omega_1{}^2 a_1}{2\omega}\sin(\phi_2) + \frac{f}{2\omega}\sin(\phi_1) \tag{13c}$$

$$-(a_2\sigma_2 + \frac{pa_2}{2\omega}) = \frac{\alpha_{22}\omega_1{}^2 a_1}{2\omega}\cos(\phi_2) + \frac{f}{2\omega}\cos(\phi_1) \tag{13d}$$

From equations (13), the frequency response equation for three different cases is investigated as follows:

Case 1 (Practical case): $a_1 \neq 0$, $a_2 \neq 0$

$$\frac{\mu_1{}^2 a_1{}^2}{4} + (a_1(\sigma_1+\sigma_2) - \frac{\alpha_{13}\omega^2 a_1 a_2{}^2}{4\omega_1})^2 - \frac{\alpha_{13}{}^2\omega^4 a_1{}^2 a_2{}^4}{64\omega_1{}^2} - \frac{\alpha_{12}{}^2\omega^4 a_2{}^2}{4\omega_1{}^2} - \frac{\alpha_{13}\alpha_{12}\omega^4 a_1 a_2{}^3}{8\omega_1{}^2}\cos(\phi_2) = 0 \tag{14}$$

$$\frac{\mu_2{}^2 a_2{}^2}{4} + (a_2\sigma_2 + \frac{pa_2}{2\omega})^2 - \frac{\alpha_{22}{}^2\omega_1{}^4 a_1{}^2}{4\omega^2} - \frac{f^{\,2}}{4\omega^2} - \frac{\alpha_{22}\omega_1{}^2 a_1 f}{2\omega^2}\cos(\phi_1+\phi_2) = 0 \tag{15}$$

Case 2 (Ideal case): $a_1 = 0$, $a_2 \neq 0$

$$\frac{\mu_2{}^2 a_2{}^2}{4} + (a_2\sigma_2 + \frac{pa_2}{2\omega})^2 - \frac{f^{\,2}}{4\omega^2} = 0 \tag{16}$$

Case 3 (trivial solution): $a_1 \neq 0$, $a_2 = 0$

$$\frac{\mu_1{}^2 a_1{}^2}{4} + a_1{}^2(\sigma_1+\sigma_2)^2 = 0 \tag{17}$$

2.3 Stability analysis

i) To study the stability of the steady state solution at the obtained fixed points of the linear system, let us consider $A_o(T_1)$ and $B_o(T_1)$ in the Cartesian form as

$$A_0 = \frac{1}{2}(p_1 - iq_1)e^{i\delta_1 T_1} \quad , \; B_0 = \frac{1}{2}(p_2 - iq_2)e^{i\delta_2 T_1} \tag{18}$$

Where p_1, p_2, q_1, q_2 are real values, where $\delta_1 = \sigma_1 + \sigma_2$, $\delta_2 = \sigma_2$. Then from equations (10), the linear form is obtained as:

$$-2i\,\omega_1 D_1 A_0 - i\,\omega_1\mu_1 A_0 + \alpha_{12}\omega^2 B_0 = 0 \tag{19a}$$

$$-2i\,\omega D_1 B_0 - i\,\omega\mu_2 B_0 + pB_0 + \alpha_{22}\omega_1^{\,2} A_0 + \frac{f}{2} = 0 \tag{19b}$$

Substituting equation (18) into equations (19), and separating the real and imaginary parts yields to:

$$\dot{p}_1 = -\frac{\mu_1}{2} p_1 - (\sigma_1 + \sigma_2) q_1 - \frac{\alpha_{12}\omega^2}{2\omega_1} q_2 \tag{20a}$$

$$\dot{q}_1 = (\sigma_1 + \sigma_2) p_1 - \frac{\mu_1}{2} q_1 + \frac{\alpha_{12}\omega^2}{2\omega_1} p_2 \tag{20b}$$

$$\dot{p}_2 = -\frac{\alpha_{22}\omega_1^{\,2}}{2\omega} q_1 - \frac{\mu_2}{2} p_2 - (\sigma_2 + \frac{P}{2}) q_2 \tag{20c}$$

$$\dot{q}_2 = \frac{\alpha_{22}\omega_1^{\,2}}{2\omega} p_1 + (\sigma_2 + \frac{p}{2}) p_2 - \frac{\mu_2}{2} q_2 + \frac{f}{2\omega} \tag{20d}$$

The stability of the linear solution is determined by the zeros of the characteristic equation:

$$\begin{vmatrix} \rho_{11}-\lambda & \rho_{12} & 0 & \rho_{14} \\ \rho_{21} & \rho_{22}-\lambda & \rho_{23} & 0 \\ 0 & \rho_{32} & \rho_{33}-\lambda & \rho_{34} \\ \rho_{41} & 0 & \rho_{43} & \rho_{44}-\lambda \end{vmatrix} + \frac{f}{2\omega} = 0 \tag{21}$$

This can be simplified to obtain the eigenvalue equation

$$\lambda^4 + r_1\lambda^3 + r_2\lambda^2 + r_3\lambda + r_4 = 0 \tag{22}$$

where $\rho_{ij}, r_1, r_2, r_3, r_4$ are constants given in Appendix-1.

By applying Routh-Hurwitz criterion [39,40], to investigate the stability of the steady-state solution, we find the necessary and sufficient conditions for all the roots of Eq. (22) satisfies the following relations $r_1 > 0, r_1 r_2 - r_3 > 0, r_3(r_1 r_2 - r_3) - r_1^{\,2} r_4 > 0, r_4 > 0$ and possess negative real parts.

ii) Now to study the stability of the steady-state solution at the obtained fixed points of the nonlinear system, let us consider

$$a_1 = a_{10} + a_{11}, a_2 = a_{20} + a_{21}, \phi_1 = \phi_{10} + \phi_{11}, \phi_2 = \phi_{20} + \phi_{21} \tag{23}$$

Where $a_{10}, a_{20}, \phi_{10}$ and ϕ_{20} are the solutions of equations (13) and $a_{11}, a_{21}, \phi_{11}$, and ϕ_{21} are perturbations which are assumed to be small compared to $a_{10}, a_{20}, \phi_{10}$, and ϕ_{21}. Substituting equation (23) into equations (12) and expanding for small $a_{11}, a_{21}, \phi_{11}$ and ϕ_{21} with keeping the linear terms only, we get:

$$\dot{a}_{11} = -\left(\frac{\mu_1}{2} + \frac{\alpha_{13}\omega^2 {a_{20}}^2 \sin(\phi_{20})\cos(\phi_{20})}{4\omega_1}\right)a_{11} + \left(\frac{\alpha_{13}\omega^2 \sin(\phi_{20})(1+a_{10}a_{20}\cos(\phi_{20})}{2\omega_1}\right)a_{21}$$
$$+\left(\frac{\alpha_{13}\omega^2 a_{10}{a_{20}}^2}{4\omega_1}(\cos^2(\phi_{20}) - \sin^2(\phi_{20}) + \frac{\alpha_{12}\omega^2 a_{20}\cos(\phi_{20})}{2\omega_1}\right)\phi_{21} \quad (24a)$$

$$\dot{\phi}_{11} = (\frac{\alpha_{22}{\omega_1}^2\cos(\phi_{20})}{2a_{20}\omega})a_{11} - (\frac{f\ \sin(\phi_{10})}{2a_{20}\omega})\phi_{11} + (\frac{\sigma_2}{a_{20}} + \frac{p}{2a_{20}\omega})a_{21} + (\frac{\alpha_{22}{\omega_1}^2 a_{10}\sin(\phi_{20})}{2\omega a_{20}})\phi_{21} \quad (24b)$$

$$\dot{a}_{21} = -(\frac{\alpha_{22}{\omega_1}^2\sin(\phi_{20})}{2\omega})a_{11} + (\frac{f\ \cos(\phi_{10})}{2\omega})\phi_{11} - \frac{\mu_2}{2}a_{21} - (\frac{\alpha_{22}{\omega_1}^2\ a_{10}\cos(\phi_{20})}{2\omega})\phi_{21} \quad (24c)$$

$$\dot{\phi}_{21} = \left(\frac{\sigma_1+\sigma_2}{a_{10}} - \frac{\alpha_{13}\omega^2 {a_{20}}^2}{4\omega_1 a_{10}} + \frac{\alpha_{13}\omega^2 {a_{20}}^2(1-2\sin^2(\phi_{20}))}{8\omega_1 a_{10}}\right)a_{11} - \left(\frac{\alpha_{13}\omega^2\ a_{10}{a_{20}}^2\sin(\phi_{20})\cos(\phi_{20})}{2\omega_1 a_{10}}\right)\phi_{21}$$
$$+\left(-\frac{\alpha_{13}\omega^2 a_{10}a_{20}}{2\omega_1 a_{10}} + \frac{\alpha_{13}\omega^2 a_{10}a_{20}(1-2\sin^2(\phi_{20}))}{4\omega_1 a_{10}}\right)a_{21} \quad (24d)$$

The stability of the steady state solution in this case depends on the eigenvalues of the following square determinant

$$\begin{vmatrix} \zeta_{11}-\lambda & 0 & \zeta_{13} & \zeta_{14} \\ \zeta_{21} & \zeta_{22}-\lambda & \zeta_{23} & \zeta_{24} \\ \zeta_{31} & \zeta_{32} & \zeta_{33}-\lambda & \zeta_{34} \\ \zeta_{41} & 0 & \zeta_{43} & \zeta_{44}-\lambda \end{vmatrix} = 0 \quad (25)$$

Where λ denotes the eigenvalues of the above determinant and ζ_{ij} are constants that given in Appendix-1. According to Routh-Huriwitz criterion, the necessary and sufficient conditions for the steady-state solution to be stable is $r_1 > 0, r_1 r_2 - r_3 > 0, r_3(r_1 r_2 - r_3) - r_1^2 r_4 > 0, r_4 > 0$, and the roots of equation (25), possess negative real parts.

3 Results and Discussion

In this section, we will report and discuss numerical solutions of the frequency response equations and the effects of different parameters on the steady state solution, the results are shown graphically near the solution of the simultaneous resonance case.

For the practical case $(a_1 \neq 0, a_2 \neq 0)$, the frequency response equations are given by equations (14) and (15) and solved numerically at the previous selected values. As shown in Fig. (4a), the curve of the steady state amplitude a_1 of the rotating beam against the detuning parameters σ_1 is bent to the left denoting softening effect with multi-valued and jump phenomenon. Also the observed relation between the amplitude of a_1 response and σ_1 detuning is nonlinear. It should be noted that the shift to the right is due to an apparent increase in the natural frequency with increasing nonlinearity [37]. Thus, the jump phenomenon is a nonlinear phenomenon, which takes place for soft as well as hard springs (for negative or positive values of any nonlinear parameter). As the frequency is decreased, the response amplitude jumps to a lower amplitude for a soft spring and to a higher amplitude for a hard spring.

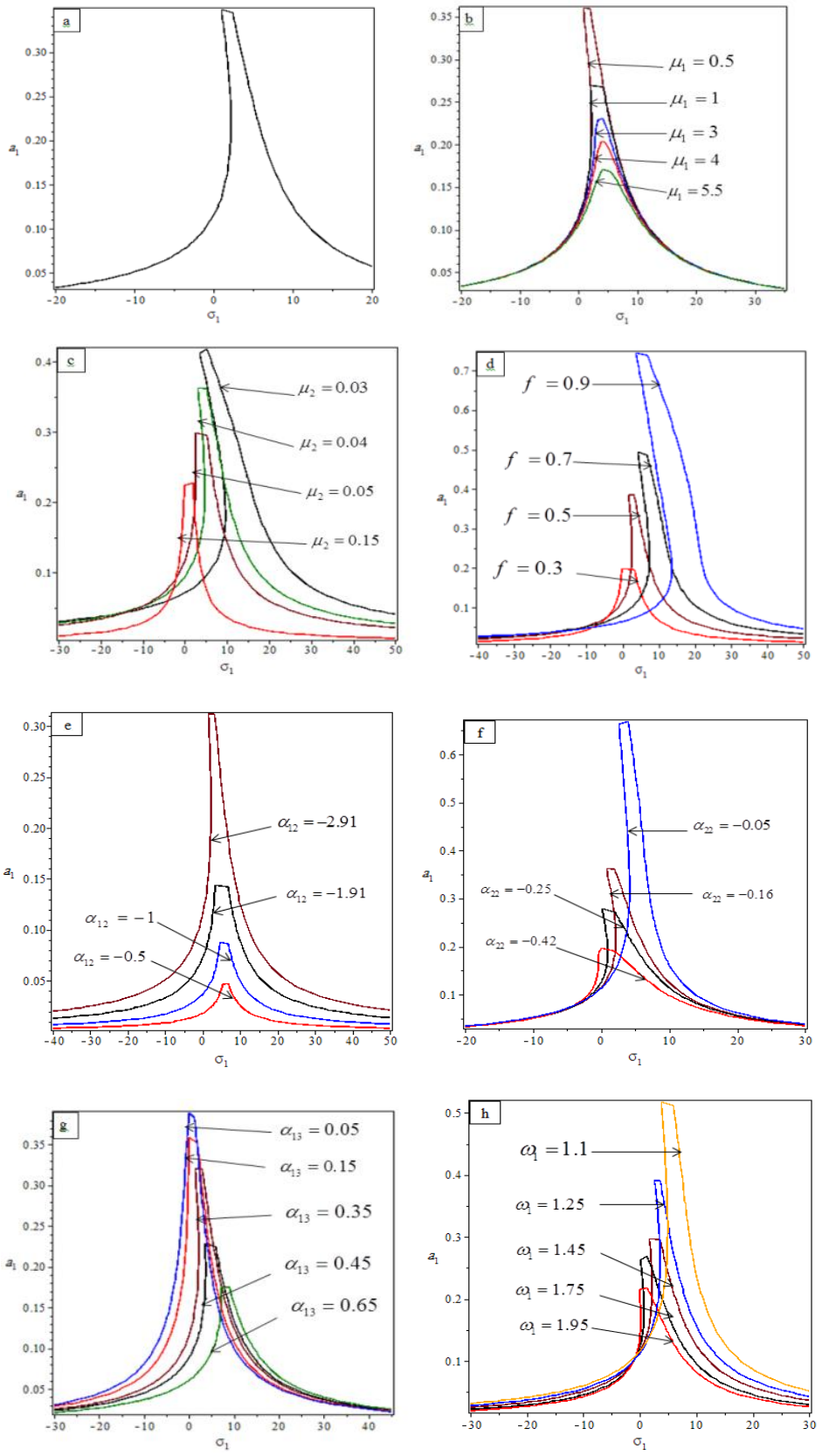

Fig. 4. Effects of different parameters on the detuning parameter (a_1 against σ_1)

The effects of different parameters on the steady-state amplitude a_1 are obtained as shown in Fig. (4b,…, 4h), and discussed. From Fig. 4b and 4e, the steady state amplitude a_1 is a monotonic decreasing function of the parameters μ_1 and α_{12} of the beam with increasing in the instability region for α_{12} and all the curves bent to the left. For the hub damping coefficient μ_2 as shown in Fig. 4c, the steady state amplitude a_1 is a monotonic decreasing and the curves are shifted to the left with decreasing in the instability region. From these figures it can be noticed that the parameters of $\mu_1, \alpha_{12}, \mu_2$ are inversely proportional of the amplitude of a_1. Also as shown in Fig. 4d, the steady state amplitude a_1 is a monotonic increasing function of f with increasing in the instability region and the curves are shifted to the left because the rotating of the hub by the external force. From Fig. 4g, the steady state amplitude a_1 is a monotonic decreasing function of the parameter α_{13} and the curves are shifted to the right. For the parameter α_{22} as shown in Fig. 4f, the steady state amplitude a_1 is a monotonic increasing and all the curves bent to the left**.** For the natural frequency of the rotating beam ω_1 as shown in Fig. 4h, the steady state amplitude a_1 is a monotonic decreasing function and all the curves bent to the left with decreasing in the instability region**.** For the parameters $\mu_1, \mu_2, f, \omega_1$ and α_{22} the frequency response curves are bent to the left and have a softening effect because the jumps take place in the opposite direction. The jumps are a consequence of the multivalued of the frequency response, which is in turn due to the domination of the negative values of the nonlinearity parameters of α_{12}, α_{22}.

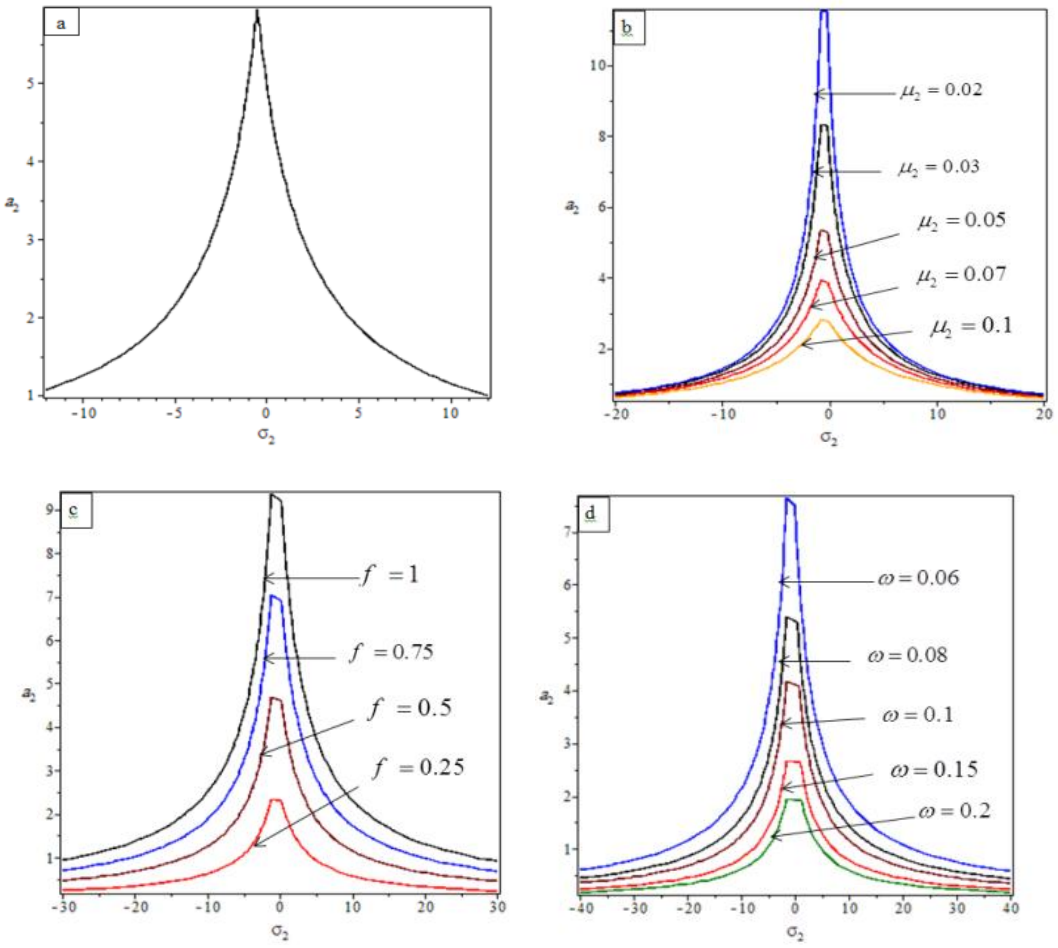

Fig. 5. Effects of different parameters on the detuning parameter (a_2 against σ_2)

Also, the steady state amplitude a_2 of the hub system against detuning parameter σ_2 is obtained as shown in Fig. 5a**.** From Fig. 5b and 5d, the steady state amplitude a_2 is a monotonic decreasing function of the parameters μ_2 and ω with decreasing in the instability region for ω, which is mean the hub will be stable. For the excitation force f the steady state amplitude a_2 is a monotonic increasing function of the force f with increasing in the instability region as shown in Fig. 5c, that means the hub is unstable for big values of the excitation force f .

Finally the parameters α_{14}, α_{21} and α_{23} for the quadratic terms in the equations of the beam and hub have no significant effect on the vibration of the composite system and on the steady state amplitudes of the system, that means the occurrence of saturation phenomena is obtained.

4 Conclusions

The vibrations of a second order, non-linear of the hub system and a flexible composite thin-walled beam are investigated. The dynamics of the rotating cantilever beam in the absence of the acceleration of the hub is considered. The system governing equations indicate a slight difference between ω_1 and ω .The amplitude-phase modulating equations of both the beam and hub oscillations modes are obtained by applying the multiple scale perturbation method. The algebraic equations that describe the system steady state amplitudes are obtained as a function of the system parameters, and the detuning parameters σ_1 and σ_2 .The effects of system parameters on the steady state amplitudes of vibrating system are investigated using frequency response curves and reported. The conclusions that we got were as follows:

1. The steady state response for the non-resonant system at some practical values of the equations parameters. The rotating beam z is about 3% of the external excitation force (f), and the amplitude is decreasing with some chaos. The amplitude of the hub system ψ for is about 50% of the external excitation force (f).
2. The worst resonance case of the rotating beam and the hub system occurs at simultaneous primary and internal resonance case $\omega = \omega_1, \Omega \cong \omega$ where the steady state response of the rotating beam is about 2000% of the external excitation force and the amplitude of the hub system is about 120% of the external excitation force .
3. The steady-state amplitude a_1 is a monotonic decreasing function of the parameters $\mu_1, \alpha_{12}, \alpha_{13}$ and ω_1 of the beam with increasing in the instability region for α_{12} and decreasing in the instability region for ω_1 .
4. The steady-state amplitude a_1 is a monotonic decreasing function of the parameter μ_2 of the hub with decreasing in the instability region, and monotonic increasing function of the parameters α_{22} and the excitation force (f) of the hub with increasing in the instability region for (f).
5. For increasing values of the parameters μ_2, f and α_{13}, the frequency response curves are shifted to left for μ_2 and shifted to the right for f and α_{13}.
6. The steady state amplitude a_2 is a monotonic decreasing function of the parameters μ_2 and ω of the hub with decreasing in the instability region for ω.

7. The steady state amplitude a_2 is a monotonic increasing function of the excitation force f of the hub with increasing in the instability region for f .

8. In a comparison with previous work [35], practical analysis of system dynamics started for free vibrations of the non-moving and non-rotating structure. The author studied the natural frequency of the system with respect to the relative hub inertia. For the forced vibrations are examined under periodic excitation f and without translational motion $\ddot{\xi} = 0$. Dynamics for the structure is typically linear and the resonance for the hub-beam combined system occurs at $\omega \approx 2.47$. The oscillations of the hub, from the resonance observed around the natural frequency, were very small (close to zero), and the frequency, which corresponds to the natural frequency of the separated cantilever beam, hub vibrations are suppressed but beam vibrations also remain small. In this paper, a first order approximation solution of the beam and hub is obtained. The solution is acquired by applying multiple scale method [37,38]. The system frequency response curves are studied around simultaneous of primary and internal resonance case. The steady state amplitudes of the rotating beam and hub are plotted at different values of system parameters. The effects of system parameters on the steady state amplitudes and the multi-jump phenomenon are reported numerically.

Now, we are interested in studying the vibration of a composite system consisting of a rotating rigid hub and a flexible thin-walled beam subject the forced vibrations under periodic excitation f and translational motion as a future work.

Competing Interests

Authors have declared that no competing interests exist.

References

[1] Subrahmanyam K, Kulkarni S, Rao J. Coupled bending-torsion vibrations of rotating blades of asymmetric aerofoil cross section with allowance for shear deflection and rotary inertia by use of the Reissner method. Journal of Sound and Vibration. 1981; 75(1):17-36.

[2] Dokumaci E. An exact solution for coupled bending and torsion vibrations of uniform beams having single cross-sectional symmetry. Journal of Sound and Vibration. 1987; 119(3):443-449.

[3] Bishop R, Cannon S, Miao S. On coupled bending and torsional vibration of uniform beams. Journal of Sound and Vibration. 1989; 131(3):457–464.

[4] Vasiliev V. Mechanics of composite structures. CRC Press.1993; 1st ed.

[5] Lee Y, Sheu J. Free vibrations of a rotating inclined beam. Journal of Appl. Mech. 2007; 74:406-414.

[6] Wen L, Kuo H. Free vibration analysis of rotating Euler beams at high angular velocity. Journal of Computers and Structures. 2010; 88:991-1001.

[7] Kamel M, Amer Y. Response of parametrically excited one degree of freedom system with nonlinear damping and stiffness. Physica Scripta. 2002; 66:410–416.

[8] Kamel M, Eissa M, Al-mandouh A. The response and stability of a rotor arm simulated by a cantilever beam. International Journal of Robotics Research and Development. 2014; 4:1-16.

[9] Nayfeh A, Nayfeh S. Non-linear normal modes of a continuous system with quadratic nonlinearities. Journal of Vibration and Acoustics. 1994; 117:199–205.

[10] Pesheck E, Pierre C, Shaw S. Modal reduction of a non-linear rotating beam through normal modes. Journal of Vibration and Acoustics. 2002; 124:229–236.

[11] Nayfeh A, Chin C, Nayfeh S. Non-linear normal modes of a cantilever beam. Journal of Vibration and Acoustics. 1995; 117:477–481.

[12] Petrov E, Ewins D. Effects of damping and varying contact area at blade-disk joints in forced response analysis of bladed disk assemblies. Journal of Turbomachinery. 2006; 8(2):403- 410.

[13] He B, Ouyang H, Ren X. Dynamic response of a simplified turbine blade model with under-platform dry friction dampers considering normal load variation. Applied Sciences. 2017; 7(3):228.

[14] Qin Z, Han Q, Chu F. Bolt loosening at rotating joint interface and its influence on rotor dynamics. Engineering Failure Analysis. 2016; 59:456–466.

[15] Qin Z, Yang Z, Zu J. Free vibration analysis of rotating cylindrical shells coupled with moderately thick annular plates. International Journal of Mechanical Sciences. 2018; 142(143):127–139.

[16] Li B, Ma H, Yu X. Nonlinear vibration and dynamic stability analysis of rotor-blade system with nonlinear supports. Archive of Applied Mechanics. 2019; 89(7):1375-1402.

[17] Cao D, Gong X, Wei D. Nonlinear vibration characteristics of a flexible blade with friction damping due to tiprub. Shock and Vibration. 2011; 18(1–2):105–114.

[18] Cao D, Liu B, Yao M. Free vibration analysis of a pretwisted sandwich blade with thermal barrier coating layers. Science China. Technological Sciences. 2017; 60(11):1747-1761.

[19] Das K, Ray C, Pohit G. Large amplitude free vibration analysis of a rotating beam with non-linear spring and mass system. Journal of Vibration and Control. 2005; 11(12):1511-1533.

[20] Xue X, Tang J. Vibration control of nonlinear rotating beam using piezoelectric actuator and sliding mode approach. Journal of Vibration and Control. 2008; 14(6):885-908.

[21] Pohit G, Mallik A, Venkatesan C. Free out-of-plane vibration of a rotating beam with non-linear elastomeric constraints. Journal of Sound and Vibration. 1999; 220(1):1–25.

[22] Pohit G, Venkatesan C, Mallik A. Elastomeric damper model and limit cycle oscillation in bearingless helicopter rotor blade. Journal of Aircraft. 2000; 37(5):923–926.

[23] Pohit G, Venkatesan C, Mallik A. Influence of non-linear elastomer on isolated lag dynamics and rotor/fuselage aeromechanical stability. Journal of Aircraft. 2004; 41(6):1449– 1464.

[24] Avramov K, Pierre C, Shyriaieva N. Flexural-flexural-torsional nonlinear vibrations of pre-twisted rotating beams with asymmetric cross-sections. Journal of Vibration and Control. 2007; 13(4):329–364.

[25] Avramov K, Galas O, Morachkovskii O, Pierreñ C. Analysis of flexural- flexural torsional nonlinear vibrations of twisted rotating beams with cross-sectional deplanation. Strength of Materials. 2009; 41(2):200-208.

[26] Dakel M, Baguet S, Dufour R. Steady-state dynamic behavior of an on-board rotor under combined base motions. Journal of Vibration and Control. 2014; 2254–2287.

[27] Arvin H, Bakhtiari-Nejad F. Nonlinear free vibration analysis of rotating composite Timoshenko Beams. Compos Struct. 2013; 96:29–43.

[28] Georgiades F, Latalski J, Warminski J. Equations of motion of rotating composite beam with a non-constant rotation speed and an arbitrary preset angle. Meccanica. 2014; 49:1838-1858.

[29] Luat DT, Thom DV, Thanh TT, Minh PV, Ke TV, Vinh PV. Mechanical analysis of bi-functionally sandwich nanobeams. Advances in Nano Research. 2021; 11(1):55- 71.

[30] Thom DV, Doan DH, Minh PV, Tung NS. Finite element modelling for vibration response of cracked stiffened FGM plates. Vietnam Journal of Science and Technology. 2020; 58(1):119-129.

[31] Wang B, Li XF. Flexoelectric effects on the natural frequencies for free vibration of piezoelectric nanoplates. J. Appl. Phys. 2021; 129(3).
DOI: 10.1063/5.0032343

[32] Duc DH, Thom DV, Cong PH, Minh PV, Nguyen NX. Vibration and static buckling behavior of variable thickness flexoelectric nanoplates. Mechanics Based Design of Structures and Machines; 2022.
DOI:10.1080/15397734.2022.2088558

[33] Nguyen HN, Nguyen TY, Tran KV, Tran TT, Nguyen TT, Phan VD, Do TV. A finite element model for dynamic analysis of triple-layer composite plates with layers connected by shear connectors subjected to moving load. Materials. 2019; 12(598):1-19.

[34] Tho NC, Thom DV, Cong PH, Zenkour AM, Doan DH, Minh PV. Finite element modeling of the bending and vibration behavior of three-layer composite plates with a crack in the core layer. Composite Structures. 2023; 305:116529.

[35] Warminski J, Latalski J. Dynamics of rotating thin-walled cantilever composite beam excited by translational motion. Journal of Proceedings of the Institution of Mechanical Engineers. 2016; 144:1039-1046.

[36] Warminski J, Latalski J, Rega G. Bending-twisting vibrations of a rotating hub-thin- walled composite beam system. Mathematics and Mechanics of Solids. 2017; 22(6):1303-1325.

[37] Nayfeh A, Mook D. Nonlinear oscillations. Wiley, New York; 1995.

[38] Nayfeh A. Perturbation methods. Wiley, New York; 1973.

[39] Jeltsch R, Mansour M. Stability theory. Birkhäuser Verlag; 1995.

[40] Erawaty N, Kasbawati A, Amir K. Stability analysis for routh-hurwitz condition using partial pivot. Journal of Physics: Conference Series. 2019; 1341:062017.

Appendix-1

Coefficients of equation (8a)

$$E_1=\frac{\alpha_{12}\omega^2 B_0}{\omega_1^{\,2}-\omega^2} \quad ,E_2=\frac{\alpha_{14}\omega\omega_1 A_0 B_0}{\omega_1^{\,2}-(\omega_1+\omega)^2} \quad ,E_3=\frac{\alpha_{14}\omega\omega_1 A_0 \bar{B}_0}{\omega_1^{\,2}-(\omega_1-\omega)^2} \quad ,E_4=\frac{\alpha_{13}\omega^2 A_0 B_0^{\,2}}{\omega_1^{\,2}-(\omega_1+2\omega)^2}$$

$$,E_5=\frac{\alpha_{13}\omega^2 A_0 \bar{B}_0^{\,2}}{\omega_1^{\,2}-(\omega_1-2\omega)^2}$$

Coefficients of equation (8b)

$$H_1=\frac{\alpha_{22}\omega_1^{\,2}A_0}{\omega^2-\omega_1^{\,2}} \quad ,H_2=\frac{f}{2(\omega^2-\Omega^2)} \quad ,H_3=\frac{\alpha_{21}\omega^2 A_0 B_0+\alpha_{23}\omega\omega_1 A_0 B_0}{\omega^2-(\omega_1+\omega)^2}$$

$$,H_4=\frac{\alpha_{21}\omega^2 A_0 \bar{B}_0-\alpha_{23}\omega\omega_1 A_0 \bar{B}_0}{\omega^2-(\omega_1-\omega)^2}$$

Coefficients of equation (21)

$$\rho_{11}=-\frac{\mu_1}{2} \ , \ \rho_{12}=-(\sigma_1+\sigma_2) \ , \ \rho_{14}=-\frac{\alpha_{12}\omega^2}{2\omega_1} \ , \ \rho_{21}=(\sigma_1+\sigma_2) \ , \ \rho_{22}=-\frac{\mu_1}{2} \ , \ \rho_{23}=\frac{\alpha_{12}\omega^2}{2\omega_1} \ ,$$

$$\rho_{32}=-\frac{\alpha_{22}\omega_1^{\,2}}{2\omega},\rho_{33}=-\frac{\mu_2}{2},\rho_{34}=-(\sigma_2+\frac{p}{2}),\rho_{41}=\frac{\alpha_{22}\omega_1^{\,2}}{2\omega},\rho_{43}=(\sigma_2+\frac{p}{2}),\rho_{44}=-\frac{\mu_2}{2}$$

Coefficients of equation (22)

$$r_1=\mu_2+\mu_1 \quad , \quad r_2=2\sigma_2^{\,2}+\sigma_1^{\,2}+2\sigma_1\sigma_2+\sigma_2 p+\frac{\mu_2^{\,2}+p^2+\mu_1^{\,2}+4\mu_1\mu_2+2\alpha_{12}\alpha_{22}\omega\omega_1}{4}$$

$$r_3=(\sigma_1+\sigma_2)^2\mu_2+\frac{3\mu_1\mu_2^{\,2}+8\mu_1\sigma_2^{\,2}+2\mu_1 p^2+8\mu_1\sigma_2 p+2\alpha_{12}\alpha_{22}\omega\omega_1\mu_2+2\mu_1^{\,2}\mu_2+2\alpha_{12}\alpha_{22}\omega\omega_1\mu_1}{8}$$

$$r_4=\frac{2\mu_1^{\,2}\mu_2^{\,2}+4\mu_1^{\,2}\sigma_2^{\,2}+\mu_1^{\,2}p^2+4\mu_1^{\,2}\sigma_2 p+\alpha_{12}\alpha_{22}\omega\omega_1\mu_1\mu_2}{16}+\frac{\mu_2^{\,2}(\sigma_1+\sigma_2)^2}{4}-(\sigma_1+\sigma_2)^2(\sigma_2+\frac{p}{2})^2$$

$$-\frac{(\sigma_1\sigma_2)\alpha_{12}\alpha_{22}\omega\omega_1}{2}-\frac{((\sigma_1+\sigma_2)p-\sigma_2^{\,2})\alpha_{12}\alpha_{22}\omega\omega_1}{4}+\frac{\alpha_{12}\alpha_{22}\omega\omega_1(\alpha_{22}\omega\omega_1+\mu_1\mu_2)}{16}+\frac{f}{2\omega}$$

Coefficients of equation (25)

$$\zeta_{11}=\frac{-\mu_1}{2}-\frac{\alpha_{13}\omega^2 a_{20}^{\,2}\sin(\phi_{20})\cos(\phi_{20})}{4\omega_1},\zeta_{13}=\frac{\alpha_{13}\omega^2\sin(\phi_{20})(1+\mathrm{a}_{10}\mathrm{a}_{20}\cos(\phi_{20}))}{2\omega_1}$$

$$\zeta_{14}=\frac{\alpha_{13}\omega^2\,\mathrm{a}_{10}\mathrm{a}_{20}^{\,2}\cos(2\phi_{20})}{4\omega_1}+\frac{\alpha_{12}\omega^2\,\mathrm{a}_{20}\cos(\phi_{20})}{2\omega_1},\zeta_{21}=\frac{\alpha_{22}\omega_1^{\,2}\,\mathrm{a}_{20}\cos(\phi_{20})}{2a_{20}\omega},\zeta_{22}=\frac{-f\,\sin(\phi_{10})}{2a_{20}\omega}$$

$$\zeta_{23}=\frac{\sigma_2}{a_{20}}+\frac{p}{2a_{20}\omega},\zeta_{24}=\frac{\alpha_{22}\omega_1^{\,2}\,\mathrm{a}_{10}\sin(\phi_{20})}{2a_{20}\omega},\zeta_{31}=\frac{-\alpha_{22}\omega_1^{\,2}\sin(\phi_{20})}{2\omega},\zeta_{32}=\frac{\mathrm{f}\cos(\phi_{10})}{2\omega},\zeta_{33}=\frac{-\mu_2}{2}$$

$$\zeta_{34} = \frac{-\alpha_{22}\omega_1^{\,2}\,\mathrm{a}_{10}\cos(\phi_{20})}{2\omega}, \zeta_{41} = \frac{\sigma_1+\sigma_2}{a_{10}} - \frac{\alpha_{13}\omega^2\,\mathrm{a}_{20}^{\,2}}{4a_{10}\omega_1} + \frac{\alpha_{13}\omega^2\,\mathrm{a}_{20}^{\,2}\cos(2\phi_{20})}{8a_{10}\omega_1}$$

$$\zeta_{43} = \frac{-\alpha_{13}\omega^2\,\mathrm{a}_{10}\mathrm{a}_{20}}{2a_{10}\omega_1} + \frac{\alpha_{13}\omega^2\,\mathrm{a}_{10}\mathrm{a}_{20}\cos(2\phi_{20})}{4a_{10}\omega_1}, \zeta_{44} = \frac{-\alpha_{13}\omega^2\,\mathrm{a}_{10}\mathrm{a}_{20}^{\,2}\sin(\phi_{20})\cos(\phi_{20})}{2a_{20}\omega_1}$$

Peer-review history:
The peer review history for this paper can be accessed here (Please copy paste the total link in your browser address bar)
https://www.sdiarticle5.com/review-history/99830